Blue-Green Systems

IWA PUBLISHING

Blue-Green Systems Vol 3 No 1, 107 doi: 10.2166/bgs.2021.009

Hydrological performance of lined permeable pavements in Norway

Elhadi Mohsen Hassan Abdalla[a,b,c,*], Ingrid Selseth[b], Tone Merete Muthanna[c], Herman Helness[b], Knut Alfredsen[c], Terje Gaarden[d] and Edvard Sivertsen[b]

[a] NTNU: Norges teknisk-naturvitenskapelige universitet, S.P. Andersens vei 5, Trondheim, Trondelag 7031
[b] SINTEF community, S.P. Andersens vei 3, Trondheim, Trondelag 7031, Norway
[c] Department of Civil and Environmental Engineering, The Norwegian University of Science and Technology, Andersens vei 5, Trondelag 7031, Norway
[d] Vikaune Fabrikker AS, Industriveien 3, Stjørdal, Trondelag 7500, Norway
*Corresponding author. E-mail: elhadi.m.h.abdalla@ntnu.no

IS, 0000-0001-9366-169X; TMM, 0000-0002-4438-2202; HH, 0000-0001-5579-5638; KA, 0000-0002-4076-8351; TG, 0000-0003-0025-3991; ES, 0000-0003-1968-170X

ABSTRACT

Lined permeable pavements (LPPs) are types of sustainable urban stormwater systems (SUDs) that are suitable for locations with low infiltration capacity or shallow groundwater levels. This study evaluated the hydrological performance of an LPP system in Norway using common detention indicators and flow duration curves (FDCs). Two hydrological models, the Storm Water Management Model (SWMM)-LID module and a reservoir model, were applied to simulate continuous outflows from the LPP system to plot the FDCs. The sensitivity of the parameters of the SWMM-LID module was assessed using the generalized likelihood uncertainty estimation methodology. The LPP system was found to detain the flow effectively based on the median values of the detention indicators (peak reduction = 89%, peak delay = 40 min, centroid delay = 45 min, T50-delay = 86 min). However, these indicators are found to be sensitive to the amount of precipitation and initial conditions. The reservoir model developed in this study was found to yield more accurate simulations (higher NSE) than the SWMM-LID module, and it can be considered a suitable design tool for LPP systems. The FDC offers an informative method to demonstrate the hydrological performance of LPP systems for stormwater engineers and decision-makers.

Key words: lined permeable pavement, reservoir model, sustainable urban drainage systems (SUDs), SWMM

HIGHLIGHTS

- The study evaluates the hydrological performance of a lined permeable pavement system using detention indicators and flow duration curves (FDCs).
- A simple reservoir model was developed to predict the hydrological performance of permeable pavement.
- FDCs are very useful and practical tools to demonstrate the hydrological performance of permeable pavement.

INTRODUCTION

Permeable pavements (PPs) are a type of sustainable urban stormwater systems (SUDs) that can substitute normal pavements and provide valuable environmental services. PPs reduce the amounts of stormwater runoff through soil infiltration (Winston *et al.* 2018) and enhance the quality of the treated runoff (Pilon *et al.* 2019). In addition, PPs reduce the heat island impact through evaporative cooling and reduce the amount and time of standing water that may cause odor and health issues (Kuruppu *et al.* 2019).

PPs can either be drained or undrained. Undrained PPs infiltrate the water from the surface to the native soil and can be suitable for sites with deep groundwater levels and good infiltration conditions. On the other hand, drained PPs are equipped with an underdrain pipe connected to the downstream stormwater drainage system. Furthermore, the bottom of drained PPs can either be permeable or impermeable, depending on the local site conditions. Drained PPs with an impermeable liner are lined PPs (LPPs). They are more suitable for sites with low infiltration capacity or shallow groundwater levels (Zhang & Chui 2020).

For LPP systems, the permanent reduction of flow is limited to evaporation. Brown & Borst (2015) quantified the evaporation from several LPP systems and found it to account only for 2.4–7.6% of the annual water budget.

Therefore, the hydrological benefits of LPPs are primarily expected through runoff detention, which can be expressed by several indicators such as peak flow reduction, per event volume reduction, peak delay, and centroid delay. Numerous studies have investigated the hydrological benefits of PPs in the last decades (see Drake *et al.* (2013) for review). However, only a few studies were found to investigate the performance of LPP systems (Pratt *et al.* 1995; Abbott & Comino-Mateos 2003; Støvring *et al.* 2018). Abbott & Comino-Mateos (2003) analyzed 20 rainfall–runoff events collected from an LPP site. They found the LPP to reduce rainfall peaks significantly; a rainfall with 12 mm/h intensity was found to produce a runoff with a peak of 0.37 mm/h. Similarly, Støvring *et al.* (2018) investigated the hydraulic performance of several LPP plots with different layers and equal surface areas (25 m^2 each). During a period of 12 months, they observed a total of 22 rainfall–runoff events with return periods up to 2 years. They reported peak delay values ranging from 0:39 to 3:16 h and per event volume reduction of 27–69%, demonstrating good detention capabilities of LPP systems.

It can be noted that commonly reported detention indicators in PP literature, such as peak delay and peak reduction, exhibit a wide range of values even within the same PP site. For instance, Støvring *et al.* (2018) found the peak delay of one LPP to vary between 0:05 hr and 4:02, while Winston *et al.* (2018) reported a peak reduction range of 0–100% from one PP site. These indicators are inherently sensitive to PP initial conditions (Fassman & Blackbourn 2010) and rainfall characteristics (Støvring *et al.* 2018). In the general SUD literature, many studies have suggested moving toward more robust approaches that can unambiguously demonstrate the detention performance of SUD measures. Stovin *et al.* (2017) discussed the issues regarding detention indicators in green roof studies and recommended two alternative approaches based on long-term simulations. The first approach is based on plotting the cumulative density function of detention indicators across a wide range of rainfall events, while the second approach simulates design rainfall events with different amounts and varying initial conditions to produce detention charts. Lucas & Sample (2015) modified the flow duration curve (FDC) to represent the relation between runoff values and durations when these runoff values are exceeded. They applied FDCs to evaluate different scenarios of SUD implementation in a catchment. Similarly, Hernes *et al.* (2020) applied FDCs to investigate the performance of different SUD scenarios, and they concluded the suitability of FDC as a practical measure to evaluate the hydrological performance of SUDs. Using the FDC to evaluate the performance of PP was found to be limited to few studies in the literature (Fassman & Blackbourn 2010; Brown *et al.* 2012; Winston *et al.* 2018), and no study was found to apply the FDC for LPP systems.

The derivation of FDCs requires long time series of observations. For instance, Fassman & Blackbourn (2010) utilized 2 years of measurements to derive FDCs for a PP site, while Brown *et al.* (2012) used 17 months of data to plot the FDC of PP parking lot. Alternatively, a calibrated hydrological model can be applied to simulate long time series, which is beneficial when observations are limited. Several hydrological models are applied to simulate PP systems in the literature. The most common model perhaps is the Storm Water Management Model (SWMM) (Rossman 2010).

The low impact development module of the SWMM model, hereafter referred to as the SWMM-PP model, is a simplified physically based model. It has been applied in many PP studies (Kim *et al.* 2015; Chui *et al.* 2016; Xie *et al.* 2017; Randall *et al.* 2020). Most of the studies applied the SWMM-PP model of PP using parameters selected from the SWMM manual without calibration, and only a few studies were found to evaluate the accuracy of SWMM-PP models with measured data. Randall *et al.* (2020) investigated the accuracy of the SWMM-PP model using 18 rainfall–runoff events. They found the SWMM-PP model to yield simulation with reasonable accuracy for single-peak events and to perform poorly for events with multiple peaks. Liu & Chui (2017) found the SWMM-PP model to yield accurate simulations with Nash–Sutcliffe efficiency (NSE) values above 0.9 for validation events. Likewise, Palla & Gnecco (2015) calibrated a SWMM-PP model with data of one artificial rainfall event and found the model to produce simulations with high accuracy (NSE values above 0.75).

One issue in the SWMM-PP model is the high number of parameters (15 parameters) that need careful selection through measurements and calibration. One way to reduce the number of parameters that need adjustments is through a parameter sensitivity analysis. Such an analysis is made before calibration to select the most influential parameters for calibration/measurement while assigning standard values of the insensitive ones. However, only one study was found to investigate the sensitivity of the SWMM-PP model for long-term simulation (Randall *et al.* 2020). Hence, there is a need to investigate the sensitivity of SWMM-PP parameters for event-based simulations. Alternative to SWMM-PP, models with a fewer number of parameters can be applied. Conceptual reservoir models are popular in modeling green roofs (Vesuviano *et al.* 2014). However, no study was found to investigate its applicability for LPP systems.

This study attempted to address some of the mentioned limitations, specifically by:

1. Evaluating the hydrological performance of an LPP system using different detention indicators and FDCs.
2. Evaluating the sensitivity of the SWMM-PP model parameters for event-based simulations.
3. Investigating the suitability of a simple reservoir model for LPPs.
4. Comparing the performances of the SWMM-PP model and the reservoir model.

DATA AND METHODS

Site description and data collection

The site is an active parking lot near Trondheim city in Norway. It was constructed in 2019, and the data collection started in December 2019. The site includes three plots of LPPs with different properties and two undrained pavements. Each LPP has a surface area of 100 m^2 (12.5 m width $\times$ 8 m length). Precipitation data were collected on-site using a heated tipping bucket rain gauge. The outflows from the three LPP systems were measured using a V-NOTCH weir. The water levels above the weir were measured using an ultrasonic distance sensor. These water levels were converted into flows using a calibrated rating curve. During the measurement period, 5 months were dominated by snowfalls and accumulations (January 2020–May 2020). Additionally, frequent malfunctions occurred for the precipitation gauge during June, July, and August, but the quality of measurement improved between August and December. This study has focused on measurements from one of the plots (plot 4). Plot 4 comprises an interlocking pavement layer with 80 mm thickness. About 10 mm distances were made between the interlocks to allow for water to infiltrate. A bedding layer with 30 mm thickness was placed beneath the pavement layer with a particle grading ranged between 2 and 11 mm. The base layer thickness is 100 mm with course materials (grading 4–32 mm), while the sub-base layer thickness is 250 mm (grading 20–120 mm). An impermeable liner (geotextile) was placed at the boundaries of the LPP to prohibit infiltration to the native soil. A drainage pipe with a diameter of 100 mm was placed at the bottom of the sub-base layer.

Detention metrics used in the study

During the valid measurement period between August and December 2020, 11 rainfall–runoff events were observed and considered for analysis (Table 1). Four detention metrics were calculated for each of these events: peak reduction (PR), peak delay (Pd), centroid delay (Cd), and T50 delay. The PR measures the attenuation of the peak of precipitation events, while the other three indicators measure the delay of the permeable pavement drainage outflow. The following equations were used to determine the four metrics (Equations (1)–(4)).

$$\mathrm{PR} = \frac{P_{\max} - R_{\max}}{P_{\max}} \times 100\% \tag{1}$$

$$\mathrm{Pd} = t_{R_{\max}} - t_{P_{\max}} \tag{2}$$

$$\mathrm{Cd} = t_{R_{\mathrm{centroid}}} - t_{P_{\mathrm{centroid}}} \tag{3}$$

$$\text{T50 delay} = t_{R_{50\%\text{ of rain volume}}} - t_{P_{50\%\text{ of rain volume}}} \tag{4}$$

$P_{\max}$ is the peak of the rain during the rainfall–runoff event in (mm/min). $R_{\max}$ is the peak of the PP drainage outflow during the rainfall–runoff event (mm/min). $t_{P_{\max}}$ is the time from the start of the rainfall event to the peak of the rain (min). $t_{R_{\max}}$ is the time from the start of the rainfall event to the peak of the PP drainage outflow (min). $t_{P_{\mathrm{centroid}}}$ is the time from the start of the rainfall event to the centroid of the rainfall hyetograph (min). $t_{R_{\mathrm{centroid}}}$ is the time from the start of the rainfall event to the centroid of the PP drainage outflow hydrograph (min). $t_{P_{50\%\text{ of rain volume}}}$ is the time from the start of the rainfall event to the time in which 50% of the rain amount has passed (min). $t_{R_{50\%\text{ of rain volume}}}$ is the time from the start of the rainfall event to the time in which the accumulative volume of the PP drainage outflow reaches 50% of the rain amount (min).

Hydrological models

The SWMM-PP model is a simplified physically based model. It can be also classified as a hybrid model as it combines physical-based equations (Darcy law for water percolation) and empirical power formula for underdrain flow calculations (Rossman 2010). SWMM-PP conceptualizes the PP system as three layers: surface, soil, and storage layers. The water infiltrates from the surface to the soil layer (the bedding layer in the pavement) based on the

Table 1 | Detention indicators extracted for the 11 events

Event no.	Start of rainfall–runoff event	End of rainfall–runoff event	Peak of rainfall (mm/min)	Amount of rainfall (mm)	Duration of rainfall–runoff event (min)	Pr (%)	Pd (min)	Cd (min)	T50 (min)
1	08.08.2020 14:00	08.08.2020 15:00	0.45	1.94	60	99.97	33	18	–
2	20.09.2020 09:00	20.09.2020 13:00	0.29	10.92	240	55.59	112	47	45
3	21.09.2020 16:00	22.09.2020 02:00	0.18	8.8	600	44.65	12	45	9.6
4	21.09.2020 16:00	21.09.2020 19:00	0.06	0.9	180	87.52	40	14	93.6
5	22.09.2020 14:00	22.09.2020 19:00	0.03	1.72	200	88.77	29	44	-
6	23.09.2020 17:45	23.09.2020 20:00	0.08	0.29	135	97.26	22	45	86.4
7	24.09.2020 01:00	24.09.2020 22:00	0.09	4.78	1,260	87.38	49	279	395.4
8	25.09.2020 01:00	25.09.2020 23:00	0.11	2.53	1,320	97.56	84	269	606
9	08.10.2020 14:00	08.10.2020 20:00	0.32	13.69	360	57.92	109	40	62.4
10	11.10.2020 23:00	13.10.2020 05:00	0.17	6.31	1,800	93.3	26	351	–
11	23.12.2020 05:00	23.12.2020 10:00	0.13	2.76	300	89.77	66	26	–
Median values						**88.8**	**40.0**	**45.0**	**86.4**

Pr, peak reduction; Pd, peak delay; Cd, centroid delay; T50, T50 delay.

permeability of the pavement layer. Water movement through the soil layer is modeled using the Darcy law. Water is stored permanently in the soil layer until the soil moisture content exceeds the soil field capacity. The water percolates to the storage layer after the filed capacity of the soil layer is exceeded, while the underdrain flow is determined using a power-law empirical equation that is a function of the water depth above the drainage pipe. More details about SWMM-PP equations are illustrated in the Supplementary Material.

The reservoir model (Figure 1) represents the LPP by two layers: soil and storage. Precipitation falls into the soil layer and fills the available storage ($S1$-$S0$). Water starts to infiltrate (INF) to the storage layer when the permanent storage of the soil layer ($S1$) is exceeded. The storage layer is represented by a reservoir model with two outlets: the lower outlet simulates the low flows, and the upper outlet models the high flows. The flow from the

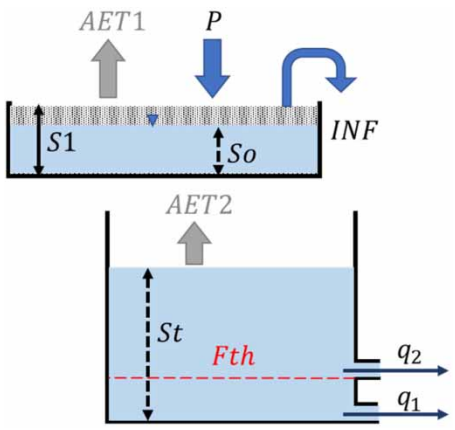

Figure 1 | Reservoir model.

upper outlet starts after the storage depth (St) exceeds a certain threshold value (Fth). The flow through the outlet is controlled by parameters $k1$ and $k2$, and the value of $k1$ which is assigned for the lower outlet is much smaller than the value of $k2$. The equations of the reservoir models are presented as follows (Equations (5)–(9)).

$$S1_t = S1_{t-1} + P_t - \mathrm{AET1}_t \tag{5}$$

$$q_1 = k1 \times \min(F\mathrm{th}, \mathrm{St}_t) \tag{6}$$

$$q_2 = k2 \times \max(0, (\mathrm{St}_t - F\mathrm{th})) \tag{7}$$

$$Q_t = q_1 + q_2 \tag{8}$$

$$\mathrm{St}_t = \mathrm{St}_{t-1} + \mathrm{INF}_t - Q_t - \mathrm{AET2}_t \tag{9}$$

The actual evapotranspiration (AET) was determined from the two tanks as a function of the potential evapotranspiration (PET) (Equations (10) and (11)). PET is the maximum evapotranspiration considering the climatological variables. In this study, the Oudin formula (Oudin *et al.* 2005) was selected to estimate the PET following the recommendation of the study of Johannessen *et al.* (2017).

$$\mathrm{AET1}_t = \frac{S0_{t-1}}{S1} \times \mathrm{PET}_t \tag{10}$$

$$\mathrm{AET2}_t = \min(\mathrm{St}_{t-1}, \mathrm{PET}_t) \tag{11}$$

In the Oudin formula, the PET is calculated from the latitude of the site and the Julian day (Equation (12)).

$$\mathrm{PET}\left(\frac{\mathrm{mm}}{\mathrm{day}}\right) = \begin{cases} 0 \text{ if } T_{\mathrm{mean}} \leq 5\,^{\circ}\mathrm{C} \\ \dfrac{Ra}{\lambda\rho} \times 0.01 \times (T_{\mathrm{mean}} + 5) \text{ if } T_{\mathrm{mean}} > 5\,^{\circ}\mathrm{C} \end{cases} \tag{12}$$

T_{mean} is the mean daily temperature (°C). The extra-terrestrial radiation Ra is calculated from the Julian day and the latitude (MJ/m^2), $1/\lambda\rho \approx 0.408$ where λ is the latent heat of vaporization (MJ/kg^1), and ρ is the volumetric mass of water (kg/m^3).

Sensitivity analysis of SWMM parameters

The number of parameters in the SWMM-PP model that needs careful selection is 15 beside the depths of the different pavement layers, while only five parameters are required for the reservoir model. Table 2 presents the models' parameters. Before the calibration of the SWMM-PP model, a sensitivity analysis was conducted using the generalized likelihood uncertainty estimation (GLUE) methodology (Beven & Binley 1992). The steps followed to conduct the GLUE methodology were based on the study of Krebs *et al.* (2016). In this study, 70,000 parameter sets were randomly selected from the parameter ranges presented in Table 2, assuming a uniform prior distribution of each parameter. These ranges were initially selected based on the recommendation of the SWMM-PP manual. Each parameter set was used to simulate a selected rainfall–runoff event, and the NSE (Nash & Sutcliffe 1970) was determined and stored. A threshold value (NSE = 0.65) was selected to separate behavioral and non-behavioral parameters. The behavioral parameters were selected to form posterior distribution for each model parameter. The Kolmogorov–Smirnov (KS) (Darling 1957) test was conducted to measure the difference between each parameter's prior and posterior distributions (Beven & Binley 1992; Krebs *et al.* 2016). The parameter is considered sensitive if the difference between the prior and posterior distributions is statistically significant based on the KS test. Event 9 was selected for the sensitivity analysis of the SWMM model parameter. This event was selected due to the long antecedent dry weather period (15 days), which allows to set the initial saturation to zero.

Model calibration

Five events were chosen for models' calibration based on the quality of the measurements. For the SWMM-PP model, the sensitive parameters were selected for calibration, while the insensitive ones were fixed to their default values, following the SWMM-PP manual. The differential evolution algorithm (DE) was used to calibrate the two models (Storn & Price 1997). The algorithm generates populations of candidate solutions by varying model parameters

Table 2 | Model parameters of the two models and the statistic *D*-value and the *p*-value from the KS test

Model	Parameter	Layer	Symbol	Lower limit	Upper limit	Selected/optimized value	*D*-value	*p*-value
SWMM[a]	Manning	Surface				0.1		
	Void fraction	Pavement	voidP	0.1	0.9	0.1	0.013	0.391
	Impervious surface fraction		Imp	0.5	1	0.9	0.018	0.109
	Permeability		Perm	5	20	20	0.153	<0.05
	Porosity	Soil	POR	0.25	0.5	0.44	0.265	<0.05
	Field capacity		FC	0.07	0.25	0.1	0.282	<0.05
	Wilting point		WP	0.01	0.06	0.05	0.118	<0.05
	Conductivity		Kc	10	1,000	1,000	0.108	<0.05
	Conductivity slope		Kcs	5	60	35	0.411	<0.05
	Suction head		Sh	1	100	50	0.011	0.575
	Void ratio	Storage	voidS	0	1	0.01	0.087	<0.05
	Flow coefficient	Drain	dCoff	0	1	1	0.092	<0.05
	Flow exponent		Dexp	0	3	0	0.252	<0.05
	Drain offset					0		
	Initial saturation	–				Varies		
Reservoir model	S1	Soil		0	30	3		
	k1	Storage		0	1	0.04		
	k2			0	1	0.004		
	Fth					2.5		
	Initial saturation	–				Varies		

[a]More details about the SWMM-PP and its parameters are presented in the Supplementary material.

within given ranges. Each population has several solutions equal to the number of model parameters multiplied by two. At each iteration, a new population is evolved from the previous one in a way that each solution of the new population is either better-off or remains the same. The algorithm was applied to optimize model parameters for each of the five events with 1,500 iterations. The best solution for each iteration was stored. The optimized 1,500 parameter sets of each of the five events were compared to find a common parameter set that produces reasonable simulations for all five events. In this study, a 'reasonable' or 'acceptable' simulation was defined based on the NSE value (NSE > 0.5), as commonly applied in the literature (Rosa *et al.* 2015; Johannessen *et al.* 2019).

A reservoir model with one outlet was used to calibrate the $k1$ and $k2$ values for the reservoir model. An event with a high amount of precipitation was used to find the optimal value of $k2$, while the value of $k1$ was optimized using the event with a low amount of precipitation. The threshold value was selected as the maximum water level in the storage tank (St) during the simulation of the low event. The maximum holding capacity ($S1$) was selected as 10% of soil layer depth following the calibration result of the SWMM model. Finally, these parameters were fixed, and each event was calibrated to find the optimal initial contents.

Continuous simulations

Precipitation and temperature data of 2017, with a one-minute time step, from the Risvollan station in the Trondheim city was used in the two calibrated models to generate 1 year of continuous outflow of the LPP from each model. In addition, a catchment with 100% impervious surface and the same area as the LPP site (8 m * 12.5 m) was modeled in the SWMM using the same climatic data to generate continuous outflow of an impermeable pavement. The distance from the Risvollan station and the LPP site is about 20 km. In the Risvollan station, climatic variables are collected and processed for a green roof site (Johannessen *et al.* 2018). Periods from 1st October to 31st March were excluded to avoid snow accumulation periods. Evapotranspiration was excluded from the event-based calibration but included in the continuous simulations. PET, calculated from the Oudin formula, was supplied to the SWMM model as an input file. It should be noted that, unlike the reservoir model, the SWMM-PP model does not account for reduced evapotranspiration due to the soil moisture deficit.

Derivation of FDCs

Simulated outflows from the two models were used to derive FDCs. The derivation of FDCs was similar to the study of Hernes *et al.* (2020). Firstly, outflow values were ranked from highest to lowest. Secondly, the probability

of exceedance (Pe_q) for each outflow value (q) was calculated, based on the value's rank, using Equation (13). Lastly, the probability of exceedance for each outflow value was converted into the duration of outflow above the outflow value $D_{\text{above } q}$, using Equation (14).

$$Pe_q = \frac{\text{rank}_q}{\max(\text{rank})} \tag{13}$$

$$D_{\text{above } q} = Pe_q * \text{simulation period } (hr) \tag{14}$$

RESULTS AND DISCUSSION

Hydrological performance of the lined permeable pavement

During the measurement period, 11 events were considered valid for analysis. For each event, peak delay, PR, centroid delay, and T50-delay were determined. Figure 2 shows an example of these indicators determined for one event, while Table 1 summarizes the indicators values for the 11 events. The median value of the PR was 89% ranging from 44.65 to 99.97%. The delay indicators' median values were 40, 45 and 86 min for the peak delay, centroid delay, and T50-delay, respectively. The median values demonstrate the good detention performance of the LPP system, which confirmed the finding of previous studies (Pratt *et al.* 1995; Abbott & Comino-Mateos 2003; Støvring *et al.* 2018). However, it can be noted that these indicators are dependent on the initial condition and the volume of rainfall events. The lowest values of the indicators were found for Event 3, which has a high precipitation amount (8.8 mm). In addition, the LPP system was believed to be wet because of the previous event (Event 2), which occurred 1 day before Event 3. On the other hand, high PR and delay indicators were obtained for Event 8, which only has a precipitation amount of 2.53 mm.

It is relatively unambiguous to determine the PR indicator within the defined time frames for the rainfall–runoff events. In contrast, several issues regarding some delay indicators were encountered. For instance, it is unclear how to determine the value of peak delay when the rainfall event has multiple peaks with the same magnitude. This can be illustrated in Figure 3, which presents a rainfall event (Event 11) with two peaks with the same value. On the other hand, to determine T50 delay, at least 50% of the rainfall should be converted to runoff within the given time frame. However, for small precipitation events and dry initial conditions, most of the water will be retained, and the amount of runoff will not reach 50% of the amount of precipitation (Events 1, 5, 10 and 11).

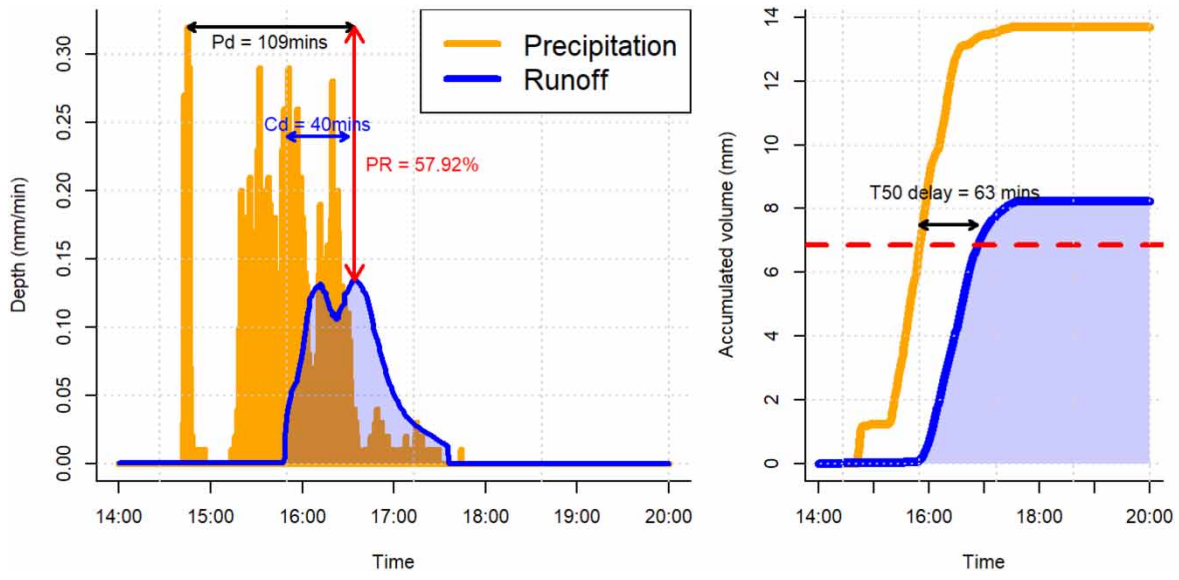

Figure 2 | Detention performance of the lined permeable pavement (plot 4) during Event 9 (October 8, 2020) using four detention metrics, which are PR (peak reduction), Pd (peak delay), Cd (centroid delay) and T50 delay. In the left figure, the blue two-sided arrow represents the value of Cd, the black two-sided arrow represents the value of Pd, and the red two-sided arrow shows the value of PR. The value of T50 delay is the difference between the accumulative curves in the right figure along the red dash line.

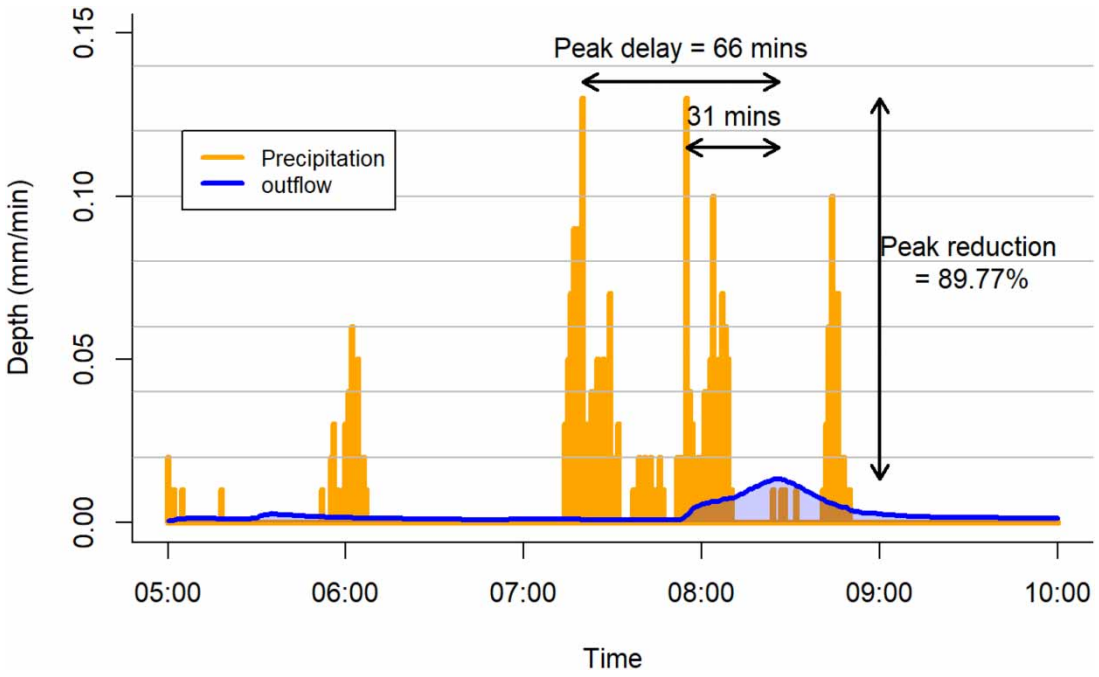

Figure 3 | Issue of determining peak delay (Event 11).

Sensitivity analysis and model calibration

5,000 parameter sets were found to be behavioral, based on the NSE values, which account for 7% of the total parameter sets. The cumulative distribution plots of the SWMM-PP parameters are presented in Figure 4, and the statistic D-value and the *p*-value from the KS-test are shown in Table 2. Based on the KS test, only three

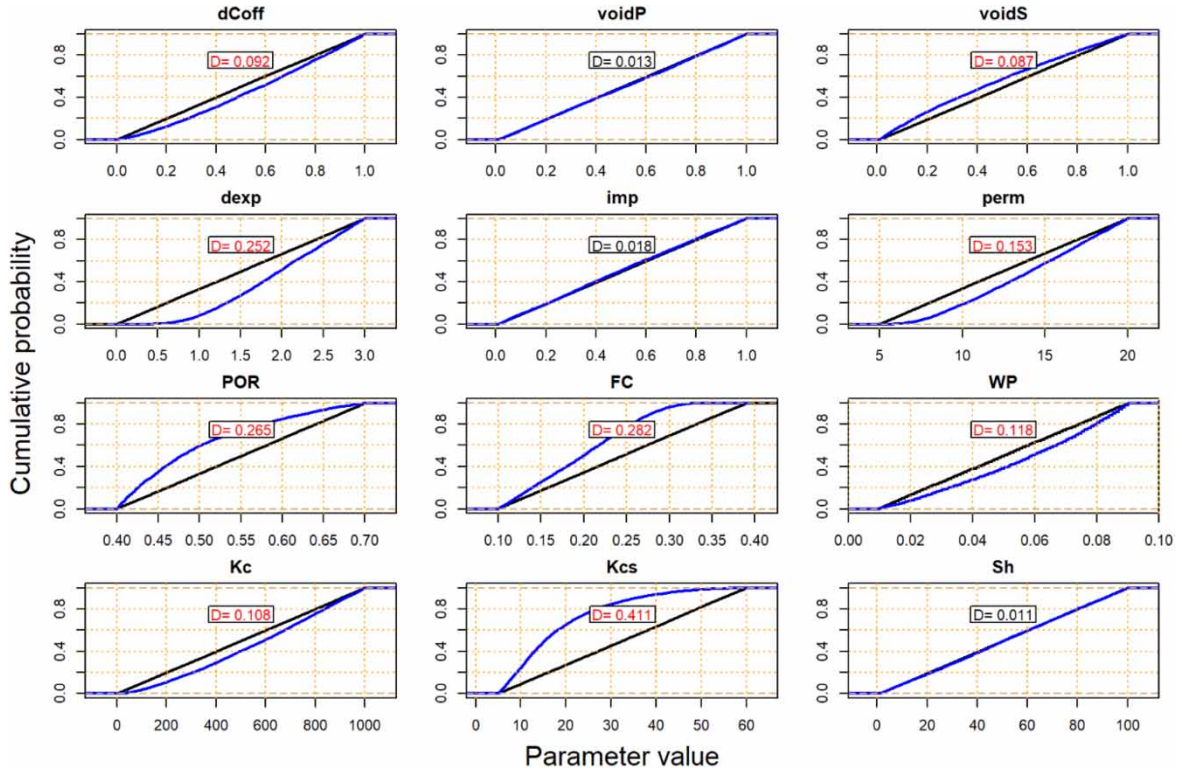

Figure 4 | Sensitivity analysis for the SWMM-PP model parameters. The black lines represent the prior distributions, while the blue lines represent the posterior distributions. *D* is the maximum distance between the prior and posterior distributions. Sensitive parameters are those with significant *D* values (colored in red) based on the KS test.

parameters of the SWMM-PP parameters are considered insensitive ($p > 0.05$). These are the void fraction of the pavement layer, the impermeable fraction of the pavement layer, and the soil layer's suction head.

The latter agrees with similar studies that found the suction head parameter to be insensitive in SWMM-LID modules (Krebs *et al.* 2016; Randall *et al.* 2020). The most sensitive parameters were found to be the hydraulic conductivity slope, the field capacity and the porosity of the soil layer. Similarly, Krebs *et al.* (2016) found all soil parameters of the SWMM-green roof model, except the suction head, to be sensitive.

The parameters of the soil layers were the most influential, followed by the parameters of the storage layers. The soil layer was considered in the SWMM-PP model to represent the bedding layer beneath the pavement interlocks. In other PP types without bedding layer (e.g. Zhang & Guo 2015), the soil layer can be eliminated from the SWMM-PP model, which reduces significantly the number of calibrated parameters and is expected to increase the sensitivity of the storage and drain parameters of the SWMM-PP model.

Model evaluations and comparisons

For the SWMM-PP model, the most optimal parameter set (highest NSE value) differed between the five selected events. Efforts were made to find a common parameter set that gives reasonable results for the five events. This was an iterative process by exploring the 1,500 parameter sets identified by the DE algorithm for each event.

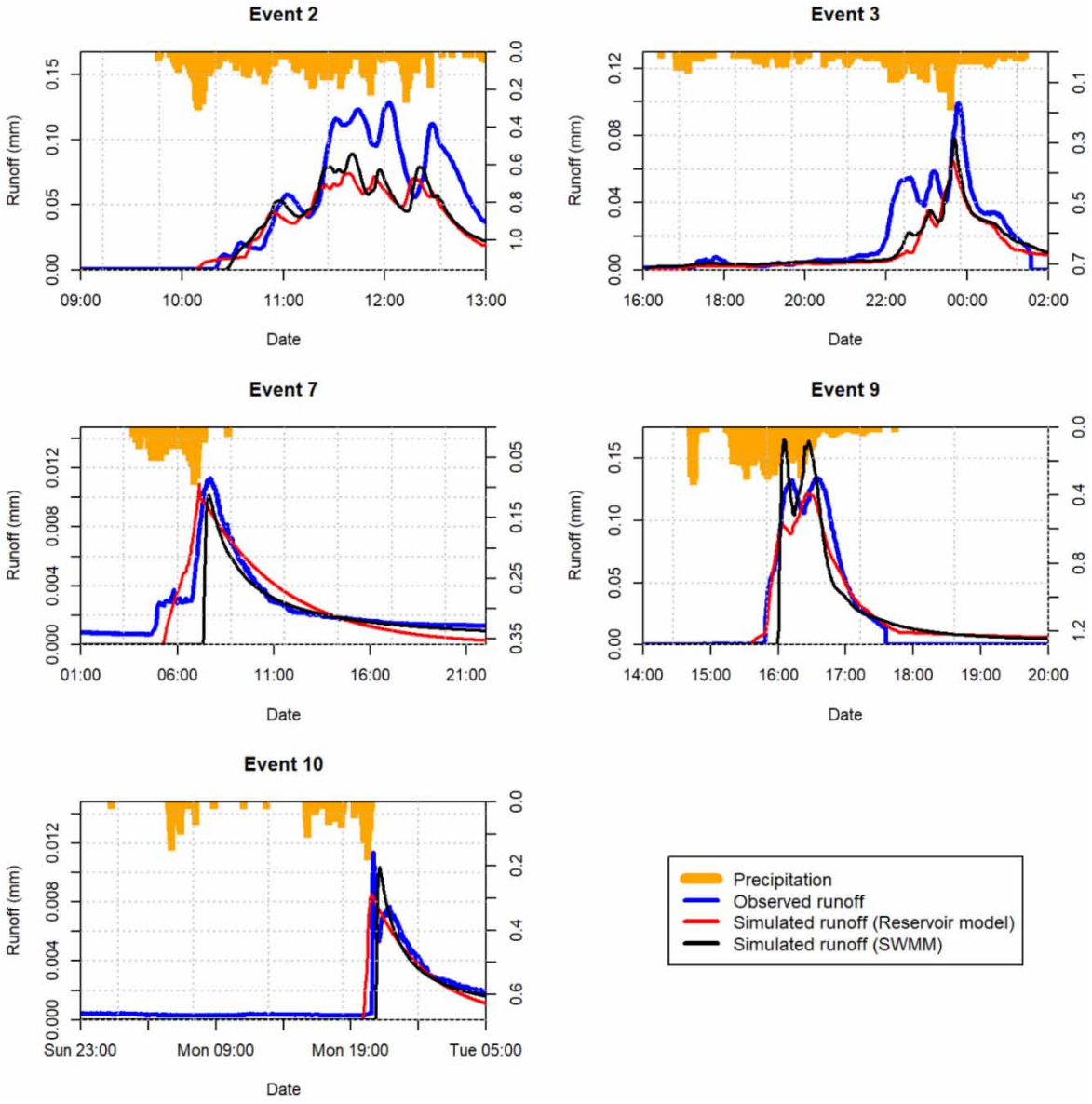

Figure 5 | Models evaluations results.

Eventually, a common parameter set was found to yield simulation with reasonable accuracy (NSE > 0.5) for the five selected events (Table 2). For the reservoir model, Event 9 was selected to find the optimal value of k2, which was found to be 0.04. The value of k2 was validated on Event 2 and found to produce a result with reasonable accuracy. Event 7 was selected to optimize the value of k1, which was validated on Event 10 and was found to equal 0.004. The maximum water level at the storage layer (St) for Event 7 was selected as the value of the flow threshold parameter (Fth). The value of S1 was taken as 10% of the soil layer, following the calibration of the SWMM-PP model. The results of the two models are illustrated in Figure 5 and Table 3.

In general, the reservoir model yielded slightly more accurate simulations (average NSE = 0.74) than the SWMM-PP model (average NSE = 0.69). The reservoir model was found to perform better (higher NSE) than the SWMM-PP model in three events (Events 7, 9, and 10), while the SWMM-PP performed slightly better in two events (Events 2 and 3). In addition, it should be emphasized that the calibration of the reservoir model, with the aim of finding a common parameter set for the five events, was much easier and faster than the SWMM-PP model calibration.

Continuous simulations and FDCs

The FDCs are presented in Figure 6. The two models produced similar permeable pavement outflows. However, it can be noted that the SWMM-PP model outflows were lower than those predicted by the reservoir model, especially during low flows. This was expected, as the SWMM model does not account for the soil moisture deficit when determining the actual evapotranspiration (Peng & Stovin 2017). In contrast, the reservoir model accounts for the soil moisture deficit (Equation (10)), which is more realistic.

The FDCs could unambiguously demonstrate the hydrological performance of LPP and provide valuable information for stormwater engineers and decision-makers. For instance, suppose that a value of 0.1 mm/min/area is a critical value that causes combined sewer overflow in this location, which can result in severe damages and

Table 3 | Models evaluation result (NSE) and estimated detention indicators by the two models

	NSE		Pr (%)		Pd (min)		Cd (min)		T50 (min)	
Event	RM	SW	RM	SW	RM	SW	RM	SW	RM	SW
2	0.61	0.68	74.24	69.18	88	91	41	42	69	62
3	0.58	0.69	63.58	56.44	2	5	64	51	70	52
7	0.80	0.55	87.88	88.7	15	44	263	368	401	-
9	0.93	0.82	62	48.43	100	79	59	58	87	87
10	0.79	0.69	94.97	93.9	18	52	473	504	-	-

RM, reservoir model; SW, SWMM-PP model.

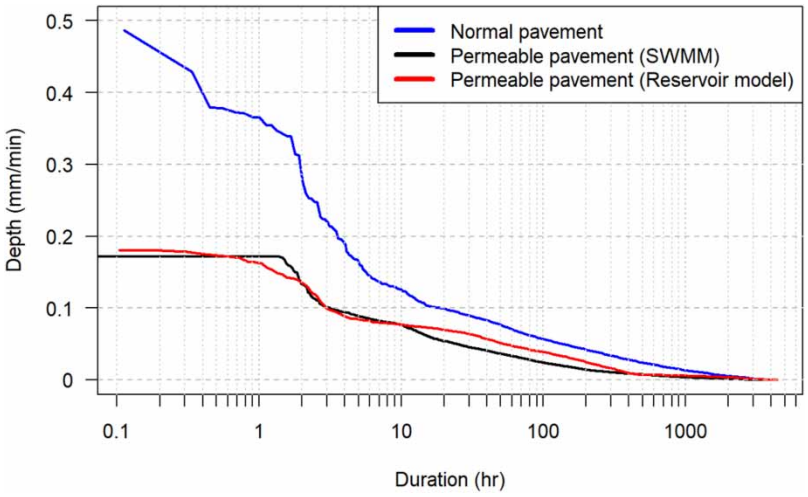

Figure 6 | FDCs of the normal pavement and the permeable pavement using the two models.

health issues. The LPP could reduce the duration of flow above this critical value from 11 h to only 3 h. Additionally, the LPP reduced the maximum outflow per unit area from nearly 0.5 mm/min to less than 0.2 mm/min.

SUMMARY AND CONCLUSION

The hydrological performance of an LPP was evaluated using several detention indicators. Issues regarding the detention indicators were presented and discussed. The study proposed the FDC as an alternative method to demonstrate the hydrological performance of LPP. The SWMM model and a reservoir model developed in this study were applied to generate continuous outflows to plot FDCs. The following conclusions can be drawn:

1. Based on the median values of detention indicators, the LPP demonstrated a good detention performance that agrees with similar studies' findings. The median value of the PR was found to be 89%. The delay indicators' median values were 40, 45, and 86 min for the peak delay, centroid delay, and T50-delay, respectively.
2. The detention indicators were found to be sensitive to the amount of precipitation and the initial condition. High values of these indicators are expected for low precipitation events and dry initial conditions.
3. Nine parameters are found to be sensitive in the SWMM-PP model for event-based simulations by following the GLUE methodology. Most of these parameters are in the soil layer (five parameters).
4. The reservoir model was found to be suitable for simulating LPP outflows. The calibration of the reservoir model, with the aim of finding a common parameter set for several events, was much easier and faster than the calibration of SWMM. Additionally, the reservoir model could yield simulations with better accuracy (higher NSE) than the SWMM model.
5. The FDC offers an informative method to demonstrate the hydrological performance of LPP systems for stormwater engineers and decision-makers.

ACKNOWLEDGEMENT

The study is part of the Drensstein project which is financed by the Research Council of Norway (grant no. 269526) and the project partners.

DATA AVAILABILITY STATEMENT

All relevant data are included in the paper or its Supplementary Information.

REFERENCES

Abbott, C. L. & Comino-Mateos, L. 2003 In-situ hydraulic performance of a permeable pavement sustainable urban drainage system. *Water and Environment Journal* **17** (3), 187–190. doi:10.1111/j.1747-6593.2003.tb00460.x.

Beven, K. & Binley, A. 1992 The future of distributed models: model calibration and uncertainty prediction. *Hydrological Processes* **6** (3), 279–298. doi:10.1002/hyp.3360060305.

Brown, R. A. & Borst, M. 2015 Quantifying evaporation in a permeable pavement system. *Hydrological Processes* **29** (9), 2100–2111. doi:10.1002/hyp.10359.

Brown, R. A., Line, D. E. & Hunt, W. F. 2012 LID treatment train: pervious concrete with subsurface storage in series with bioretention and care with seasonal high water tables. *Journal of Environmental Engineering* **138** (6), 689–697. doi:10.1061/(asce)ee.1943-7870.0000506.

Chui, T. F. M., Liu, X. & Zhan, W. 2016 Assessing cost-effectiveness of specific LID practice designs in response to large storm events. *Journal of Hydrology* **533**, 353–364. doi:10.1016/j.jhydrol.2015.12.011.

Darling, D. A. 1957 The Kolmogorov-Smirnov, Cramer-von Mises tests. *The Annals of Mathematical Statistics* **28** (4), 823–838. Available from: http://www.jstor.org/stable/2237048.

Drake, J. A. P., Bradford, A. & Marsalek, J. 2013 Review of environmental performance of permeable pavement systems: state of the knowledge. *Water Quality Research Journal of Canada* **48** (3), 203–222. doi:10.2166/wqrjc.2013.055.

Fassman, E. A. & Blackbourn, S. 2010 Urban runoff mitigation by a permeable pavement system over impermeable soils. *Journal of Hydrologic Engineering* **15** (6), 475–485. doi:10.1061/(asce)he.1943-5584.0000238.

Hernes, R. R., Gragne, A. S., Abdalla, E. M., Braskerud, B. C., Alfredsen, K. & Muthanna, T. M. 2020 Assessing the effects of four SUDS scenarios on combined sewer overflows in Oslo, Norway: Evaluating the low-impact development module of the Mike Urban model. *Hydrology Research* **51** (6), 1437–1454. doi:10.2166/nh.2020.070.

Johannessen, B. G., Hanslin, H. M. & Muthanna, T. M. 2017 Green roof performance potential in cold and wet regions. *Ecological Engineering* **106**, 436–447. doi:10.1016/j.ecoleng.2017.06.011.

Johannessen, B. G., Muthanna, T. M. & Braskerud, B. C. 2018 Detention and retention behavior of four extensive Green roofs in three Nordic climate zones. *Water* **10** (6), 671. doi:10.3390/w10060671.

Johannessen, B. G., Hamouz, V., Gragne, A. S. & Muthanna, T. M. 2019 The transferability of SWMM model parameters between green roofs with similar build-up. *Journal of Hydrology* **569**, 816–828.

Kim, H., Jung, M., Mallari, K. J. B., Pak, G., Kim, S., Kim, S., Kim, L. & Yoon, J. 2015 Assessment of porous pavement effectiveness on runoff reduction under climate change scenarios. *Desalination and Water Treatment* **53** (11), 3142–3147. doi:10.1080/19443994.2014.922286.

Krebs, G., Kuoppamäki, K., Kokkonen, T. & Koivusalo, H. 2016 Simulation of green roof test bed runoff. *Hydrological Processes* **30** (2), 250–262. doi:10.1002/hyp.10605.

Kuruppu, U., Rahman, A. & Rahman, M. A. 2019 Permeable pavement as a stormwater best management practice: a review and discussion. *Environmental Earth Sciences* **78** (10), 1–20. doi:10.1007/s12665-019-8312-2.

Liu, C. Y. & Chui, T. F. M. 2017 Factors influencing stormwater mitigation in permeable pavement. *Water* **9** (12), 988. doi:10.3390/w9120988.

Lucas, W. C. & Sample, D. J. 2015 Reducing combined sewer overflows by using outlet controls for green stormwater infrastructure: case study in Richmond, Virginia. *Journal of Hydrology* **520**, 473–488. doi:10.1016/j.jhydrol.2014.10.029.

Nash, J. E. & Sutcliffe, J. V. 1970 River flow forecasting through conceptual models part I – a discussion of principles. *Journal of Hydrology* **10** (3), 282–290. doi:10.1016/0022-1694(70)90255-6.

Oudin, L., Hervieu, F., Michel, C., Perrin, C., Andréassian, V., Anctil, F. & Loumagne, C. 2005 Which potential evapotranspiration input for a lumped rainfall-runoff model? Part 2 – towards a simple and efficient potential evapotranspiration model for rainfall-runoff modelling. *Journal of Hydrology* **303** (1–4), 290–306. doi:10.1016/j.jhydrol.2004.08.026.

Palla, A. & Gnecco, I. 2015 Hydrologic modeling of low impact development systems at the urban catchment scale. *Journal of Hydrology* **528**, 361–368. doi:10.1016/j.jhydrol.2015.06.050.

Peng, Z. & Stovin, V. 2017 Independent validation of the SWMM green roof module. *Journal of Hydrologic Engineering* **22** (9), 04017037. doi:10.1061/(ASCE)HE.1943-5584.0001558.

Pilon, B. S., Tyner, J. S., Yoder, D. C. & Buchanan, J. R. 2019 The effect of pervious concrete on water quality parameters: a case study. *Water* **11** (2), 263. doi:10.3390/w11020263.

Pratt, C. J., Mantle, J. D. G. & Schofield, P. A. 1995 UK research into the performance of permeable pavement, reservoir structures in controlling stormwater discharge quantity and quality. *Water Science and Technology* **32** (1), 63–69. doi:10.2166/wst.1995.0016.

Randall, M., Støvring, J., Henrichs, M. & Bergen Jensen, M. 2020 Comparison of SWMM evaporation and discharge to in-field observations from lined permeable pavements. *Urban Water Journal* **17** (6), 491–502. doi:10.1080/1573062X.2020.1776737.

Rosa, D. J., Clausen, J. C. & Dietz, M. E. 2015 Calibration and verification of SWMM for low impact development. *JAWRA Journal of the American Water Resources Association* **51** (3), 746–757.

Rossman, L. A. 2010 Modeling low impact development alternatives with SWMM. *Journal of Water Management Modeling* **18**, 167–182. doi:10.14796/jwmm.r236-11.

Storn, R. & Price, K. 1997 Differential evolution – a simple and efficient heuristic for global optimization over continuous spaces. *Journal of Global Optimization* **11** (4), 341–359. doi:10.1023/A:1008202821328.

Stovin, V., Vesuviano, G. & De-Ville, S. 2017 Defining green roof detention performance. *Urban Water Journal* **14** (6), 574–588. doi:10.1080/1573062X.2015.1049279.

Støvring, J., Dam, T. & Jensen, M. B. 2018 Hydraulic performance of lined permeable pavement systems in the built environment. *Water* **10** (5), 587. doi:10.3390/w10050587.

Vesuviano, G., Sonnenwald, F. & Stovin, V. 2014 A two-stage storage routing model for green roof runoff detention. *Water Science and Technology* **69** (6), 1191–1197. doi:10.2166/wst.2013.808.

Winston, R. J., Dorsey, J. D., Smolek, A. P. & Hunt, W. F. 2018 Hydrologic performance of four permeable pavement systems constructed over low-permeability soils in Northeast Ohio. *Journal of Hydrologic Engineering* **23** (4), 04018007. doi:10.1061/(asce)he.1943-5584.0001627.

Xie, J., Wu, C., Li, H. & Chen, G. 2017 Study on storm-water management of grassed swales and permeable pavement based on SWMM. *Water* **9** (11), 840. doi:10.3390/w9110840.

Zhang, K. & Chui, T. F. M. 2020 Design measures to mitigate the impact of shallow groundwater on hydrologic performance of permeable pavements. *Hydrological Processes* **34** (25), 5146–5166. doi:10.1002/hyp.13935.

Zhang, S. & Guo, Y. 2015 SWMM simulation of the storm water volume control performance of permeable pavement systems. *Journal of Hydrologic Engineering* **20** (8), 06014010. doi:10.1061/(asce)he.1943-5584.0001092.

First received 27 June 2021; accepted in revised form 26 October 2021. Available online 12 November 2021